STATISTICS, OPTIMIZATION AND INFORMATION COMPUTING
Stat., Optim. Inf. Comput., Vol. **14**, month 2025, pp 0–26.
Published online in International Academic Press (www.IAPress.org)

Enhancement of Crop Yield Prediction using an Optimised Deep Network

Sirivella Yagnasree*, Anuj Jain

School of Electronics and Electrical Engineering, Lovely Professional University, Phagwara, Punjab 144001, India

Abstract The importance of predicting crop yields lies in ensuring food security and optimising agricultural practices. Precise crop yield forecasts enable farmers and policymakers to make informed decisions about harvesting, planting, and resource allocation, ultimately affecting the availability and affordability of food. While various methods for predicting crop yields exist, they often fall short in accuracy and efficiency. This research introduces the Honey Badger-based Deep Neural Predictive Framework (HBbDNPF). The model combines the concept of Honey Badger optimisation and a deep neural network to predict different crop yields effectively. The method includes modules such as preprocessing, feature extraction, and prediction. The module reduces the complexity and enhances the accuracy of the crop yield classification. The process is tested with the Unmanned Aerial Vehicle (UAV) spectral image dataset. The model's significance improved the accuracy of the prediction and consumed less time, with an 8 ms testing time, due to the selected features. The model achieved an accuracy of 99.9%, with a precision of 99.7% and a recall rate of 99.5%. By harnessing the synergy of optimisation and deep learning, HBbDNPF empowers informed agricultural decision-making, resource allocation, and food production efficiency, contributing to global food security.

Keywords Crop Yield, Preprocessing and Classification, Honey Badger Optimisation, Deep Learning, Feature Analysis

DOI: 10.19139/soic-2310-5070-2815

1. Introduction

Agriculture is one of the essential factors for human living; it significantly influences the health and nutrition of every human being [1]. The productivity in agriculture can be improved by farmers through efficient time management and applying the correct levels of fertilisers and pesticides to crops [2]. It not only enhances productivity but also provides healthier crops. This will help the farmer acquire additional resources and store them for future use [3]. However, incorporating machine learning models into the agricultural field provides more knowledge on crop yield prediction, crop selection, soil texture prediction, disease prediction, irrigation, and price management systems [4]. These paradigms enhanced the work of the yielders in terms of economic cost and automated techniques [5]. A recent survey by the World Bank found that 50% of the food needed to be produced by 2050, based on current population growth rates. The automated agricultural system is crucial for such massive production in terms of monitoring and predicting crop yields [6]. Cost minimisation and environmental care are the core objectives of the agricultural output. Advanced prediction and management can lead to a better income for agricultural farms [7]. Techniques such as ML and statistical models were utilised for crop yield prediction in the growing season [8]. Predicting crop yield represents one of the most formidable challenges due to the diverse crop-growing processes and various environmental factors, including weather, soil, and climate. Also, the final prediction results can be identified only by the numerous independent variables [9].

Traditional statistical modelling does not always provide satisfactory results due to the complex relationship between the plants and variability [10]. Therefore, an efficient technique is needed to achieve good results in

*Correspondence to: Sirivella Yagnasree (Email: syagna100@gmail.com). PhD Scholar, School of Electronics and Electrical Engineering, Lovely Professional University, Phagwara, Punjab 144001, India.

ISSN 2310-5070 (online) ISSN 2311-004X (print)

crop yield prediction by overcoming all the critical challenges [11]. The model's functionalities are essential for predictive modelling to reach accurate forecasts [12]. In recent years, researchers have shifted their focus towards enhancing the agricultural sector and adapting neural networks to meet diverse needs within agricultural operations [13]. In the past, models such as artificial neural systems, linear regression, and vector regression were used to predict crop yields.

Additionally, to enhance the artificial neural functionalities and customised design, a modified hidden layer and learning rate are employed [14]. Additionally, the feed-forward system was also studied to predict crop yields in agricultural lands. ML and AI are the first steps that produce better outcomes in the crop yield prediction process, even for complex data [15]. The DL schemes achieved the most encouraging results in satellite image processing applications.

Several DL models were studied to get reliable predictions of crop yields. [16]. Models such as the deep neural network [17], convolutional model [18], and recurrent-based systems [19] have been researched in the past. However, the models do not achieve sufficient accuracy in prediction due to various factors, such as water level, pesticides, land cover, and fertilisers. Additionally, the model failed to reduce the relative errors, thereby degrading the prediction efficiency of crop yields [20]. To overcome these challenges of traditional crop yield prediction, this study has created an enhanced deep learning approach.

The critical contribution of the presented architecture is described as follows,

- The UAV spectral data and NDVI data are primarily collected and processed within the system.
- A novel Honey Badger-based Deep Neural Predictive Framework (HBbDNPF) architecture is developed based on Honey Badger optimisation, incorporating forecasting and classification parameters.
- The noise present in the images is eliminated during the preprocessing phase, providing refined data.
- Furthermore, efficient features were selected, and crop yields were predicted based on the honey badger's fitness process.
- Moreover, the system's efficacy is validated using metrics such as accuracy, precision, recall, and error rates.

The research paper is introduced as part of the related work in Section 2, while Section 3 highlights the challenges encountered by conventional methods. Next, the fourth section provides a detailed explanation of the proposed approach, followed by a discussion of the validation results for this innovative solution. The research paper concludes in Section 6.

2. Related Works

Some of the recent works related to our presented results are mentioned below,

Peyman et al. [21] introduced a framework that combines the outputs of multiple deep neural networks, including 3DCNN and ConvLSTM, using Bayesian Model Averaging (BMA) and a set of Copula functions. This approach provides a probabilistic estimate of soybean crop yield across three U.S. states, spanning over 100 counties. The proposed approach is more accurate when forecasting crop yield values than other deep neural networks, including ConvLSTM and 3DCNN. Additionally, it addresses the inherent uncertainties associated with model predictions. ConvLSTM and 3DCNN are computationally expensive models, particularly for long sequences, which can be slow and memory-intensive when processing large datasets, such as those used in crop yield prediction.

Maria et al. [22] proposed a temporal convolutional network method to estimate crop yields. They developed a way to use satellite images to predict how much crop will be produced in a given area. They found that the Temporal Convolutional Network (TCN) was more accurate than random forests and other methods. They tested different methods for predicting crop yields and found that TCN was the most accurate. TCN is also robust to clouds and does not require temporal compositing. TCN can still make accurate predictions even if the satellite images are partially cloudy, and they do not require preprocessing. TCNs demand an extensive dataset for practical training, which may be challenging to procure for specific tasks. This is because time series data is often not readily available, and the process is time-consuming.

Martin et al. [23] utilised machine learning techniques to predict crop harvests using weather data and shared insights regarding production trends. They aggregated weather data and crop yield information for Irish potatoes

and maise from diverse sources. The collected data underwent examination through Polynomial Regression, Support Vector Regressor, and Random Forest. The collected data was analysed. Predictors used in this analysis included rainfall and temperature. After training and testing the models, it was determined that the Random Forest model was the most suitable for early prediction of crop yields. The researchers successfully pinpointed the ideal weather conditions for each specific crop. Random forests are computationally demanding, particularly when applied to large datasets. Additionally, they can present difficulties in terms of interpretation.

Guanyuan and Bruno [24] have used GCVI and CDI to predict corn yield using remote sensing and a process-based crop model. To calculate the CDI for each field, they acquired high-resolution digital elevation models, climate data, and soil data. They executed the SALUS model, which is a process-based crop model. It was observed that integrating aggressive CDI into the model resulted in improved prediction accuracy, particularly during years characterised by dry conditions. The prediction made at the start of the growing season, combining GCVI and CDI, outshone the later forecast that solely relied on GCVI. The projections made early in the season, when the crop is still small, were more accurate when the CDI was included in the model. GCVI and CDI are sensitive to atmospheric conditions, such as cloud cover and atmospheric moisture. This can make it difficult to accurately estimate the greenness or density of a canopy under certain conditions, leading to inaccurate crop yield predictions.

Jian et al. [25] investigated the influence of different time intervals and temporal variations in Leaf Area Index (LAI) data on the results of a crop yield prediction model using LAI as input data. They also compared the performance of LSTM networks with other machine learning methods for yield estimation. The accuracy of the results did not improve as the step size and data volume increased. LSTM networks can improve yield accuracy, even when using a single input factor, such as LAI. It only considers leaf area index as an input factor, so it is not as accurate as models that consider other factors, such as soil moisture, temperature, and pests.

Jovanik et al. [32] introduced the weighted agonistic neural network to predict the crop yield. The model is tested on the real-world crops dataset. The significant potential of the model lies in its lightweight architecture, achieved through optimised parameters. It attained an average of 88.65% of the R2 values and the mean absolute error. The model improved the importance of features and prediction performance. However, the model exhibits higher costs and longer generation times.

Chandan Kumar et al. [33] explored five different machine learning models, including random forest, support vector machine, nearest neighbour, and neural network architecture, to predict corn yield. The model used seven different vegetation indices to predict crop yield. The models effectively predicted the multistage crop yield with limited trained data. However, the prediction result of the random forest is not good.

Shuaipeng Fei et al. [34] designed an ensemble model that fuses multisensory data from UAVs for yield prediction in wheat. Here, the prediction is carried out based on various features, including crop height, texture, and vegetation indices. The results demonstrated that the model achieved high prediction accuracy and was suitable for early corn yield analysis. However, the model's stability is poor. Juan Skobalski et al. [35] developed a transfer learning approach for segregating genotypes and predicting soybean yield. The trials of this method were conducted based on data collected from Argentina and the United States. Transfer learning has demonstrated its adaptability in making real-world predictions. However, the process can be enhanced by incorporating climate and soil data into the analysis. The overall disadvantages and merits of the related articles are summarised in Table 1.

3. System Model and Problem Statement

Predicting crop yields is a crucial process for decision-makers at both regional and national levels, enabling them to make informed decisions that directly impact the well-being of communities. It also helps farmers plan their crops, including which areas and when to plant them. However, predicting various climatic, soil, and weather parameters is a complex process. Different crop-yielding models have been established in the past. However, they achieved poor accuracy due to the insufficient features, which resulted in a cost-effective solution for the agricultural sector. Additionally, the methods require more extensive data training to achieve improved accuracy results. A novel study has been conducted to explore the motivation behind these issues in the present research.

Table 1. Summary of state-of-the-art approaches

Author	Method	Advantages	Disadvantages
Peyman et al. [21]	3DCNN, Bayesian Model and ConvLSTM	The proposed approach is more accurate.	Computationally expensive and slow
Maria et al. [22]	Temporal convolutional network method	It is robust to clouds and does not require temporal compositing.	An extensive dataset for practical training, which may be challenging to procure for specific tasks
Martin et al. [23]	Polynomial Regression, Support Vector Regressor	Successfully pinpointed the ideal weather conditions for each specific crop.	Present difficulties in terms of interpretation.
Guanyuan and Bruno [24]	GCVI and CDI	Accurate prediction	Difficult to accurately estimate the greenness or density of a canopy under certain conditions, leading to inaccurate crop yield predictions
Jian et al. [25]	LSTM networks	LSTM networks can improve yield accuracy, even when using a single input factor.	The accuracy of the results did not improve as the step size and data volume increased.
Jovanik et al. [32]	Weighted agonistic neural network	The model improved the feature importance and prediction performance.	Higher cost and generation time
Chandan Kumar et al. [33]	Machine learning models	Effectively predicted the multistage crop yield with limited trained data.	The prediction result of the random forest is not good.
Shuaipeng Fei et al. [34]	Ensemble model	The results proved that the model attained high prediction accuracy and was suitable for the early corn yield analysis.	The stability of the model is poor
Juan Skobalski et al. [35]	Transfer learning approach	Better adaptability to real-world predictions	The process can be enhanced by incorporating climate and soil data

The limitations of the conventional prediction method are illustrated in Fig. 1. The expected prediction approach can yield lower accuracy in this context, resulting in unfavourable results. Consequently, identifying threats in crop yield prediction using the standard method becomes particularly challenging. Furthermore, this approach lacks an

explanatory mechanism for its detection. Given its reduced accuracy, the technique proved ineffective in threat detection.

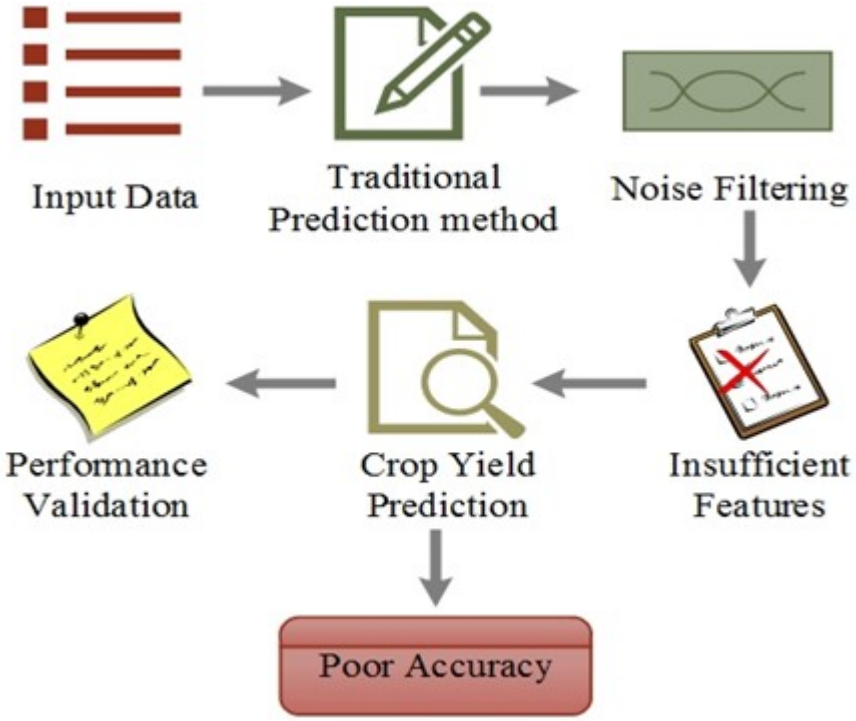

Figure 1. Challenges associated with the conventional prediction approach

4. Proposed Methodology

In this research, a novel Honey Badger-based Deep Neural Predictive Framework (HBbDNPF) is developed for the robust prediction of crop yields. The model accepted the UAV spectral data and Normalised Difference Vegetation Index (NDVI) data on crop yield prediction. Initially, the images are preprocessed to eliminate redundant noise. Furthermore, the spectral, thermal, and texture features from the UV spectral image are extracted, and crop yields are predicted; the process is defined in Fig. 2.

In the proposed HBbDNP framework, the honey badger optimisation function modifies the network's hidden layers for practical feature analysis and accurate prediction.

4.1. Process of Proposed Methodology

The work combines the merits of Honey Badger optimisation and Deep learning. The proposed method begins with the initialisation of data and its subsequent training. The procedure for this proposed methodology involves five layers: the input layer, the hidden layer, the classification layer, the optimisation layer, and the output layer.

The functioning layer of the novel HBbDNPF architecture is depicted in Fig. 3. The HBbDNPF architecture combines a deep neural network with the Honey Badger Algorithm (HBA) to achieve precise crop yield predictions. The procedure commences with UAV spectral images, which undergo preprocessing to eliminate noise, normalise data, and optionally augment samples. The HBA module is essential for feature selection and hyperparameter optimisation. HBA explicitly adjusts the learning rate (range: 0.001–0.01), batch size (16–64), Number of epochs (50–200), and the Number of neurons in the fully connected layers (Dense1: 64–256, Dense2: 32–128). In

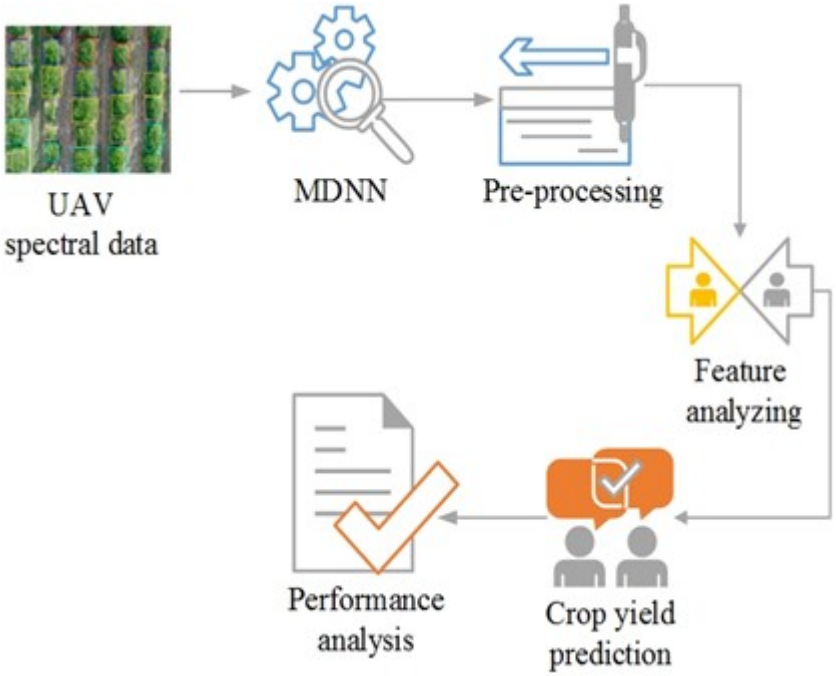

Figure 2. Proposed Methodology

the optimisation process, HBA employs a population size of 20–30 candidate solutions and executes 50–100 iterations, with a stopping condition established as either attaining convergence in validation accuracy or exceeding the maximum iteration limit. The fitness function directing HBA is the validation accuracy of the network, guaranteeing that chosen features and hyperparameters optimise prediction performance. Post-optimisation, the feature extraction module, comprising convolutional layers (Conv1: 32 filters, 3×3; Pool1: 2×2 max pooling; Conv2: 64 filters, 3×3; Pool2: 2×2 max pooling), succeeded by a flatten layer, effectively extracts hierarchical spatial and spectral patterns from the UAV images. The fully connected layers (Dense1: 128 neurons, Dense2: 64 neurons, incorporating dropout) amalgamate these parameters, while the output layer employs Softmax or Sigmoid activation to forecast crop production categories. HBbDNPF integrates HBA-driven optimisation with deep learning to reduce dimensionality, accelerate convergence, simplify computational complexity, and achieve precise crop yield predictions.

Within the HBbDNPF framework, the Honey Badger Algorithm (HBA) functions as a metaheuristic optimisation method derived from the feeding and burrowing behaviours of honey badgers. The primary function is to improve feature selection from UAV spectral images and optimise, hyperparameter tuning of the deep neural network, hence maximising prediction accuracy and reducing computational complexity. The HBA dynamically equilibrates exploration and exploitation through the following fundamental equations: during the excavation phase exploitation in Eqn. (1).

$$X_{t+1} = X_t + \beta \cdot \text{intensity} \cdot (X_{\text{best}} - X_t) \tag{1}$$

Current solution vector is exposed as X_t it encapsulates a particular configuration of neural network hyperparameters (learning rate, batch size, number of neurons, epochs) and a selection of features from UAV spectral images. The best solution of the honey badger is X_{best}, which is utilised for attaining the best accuracy, and the random factor is exposed as β

$$X_{t+1} = X_t + \alpha \cdot r \cdot (X_i - X_k) \tag{2}$$

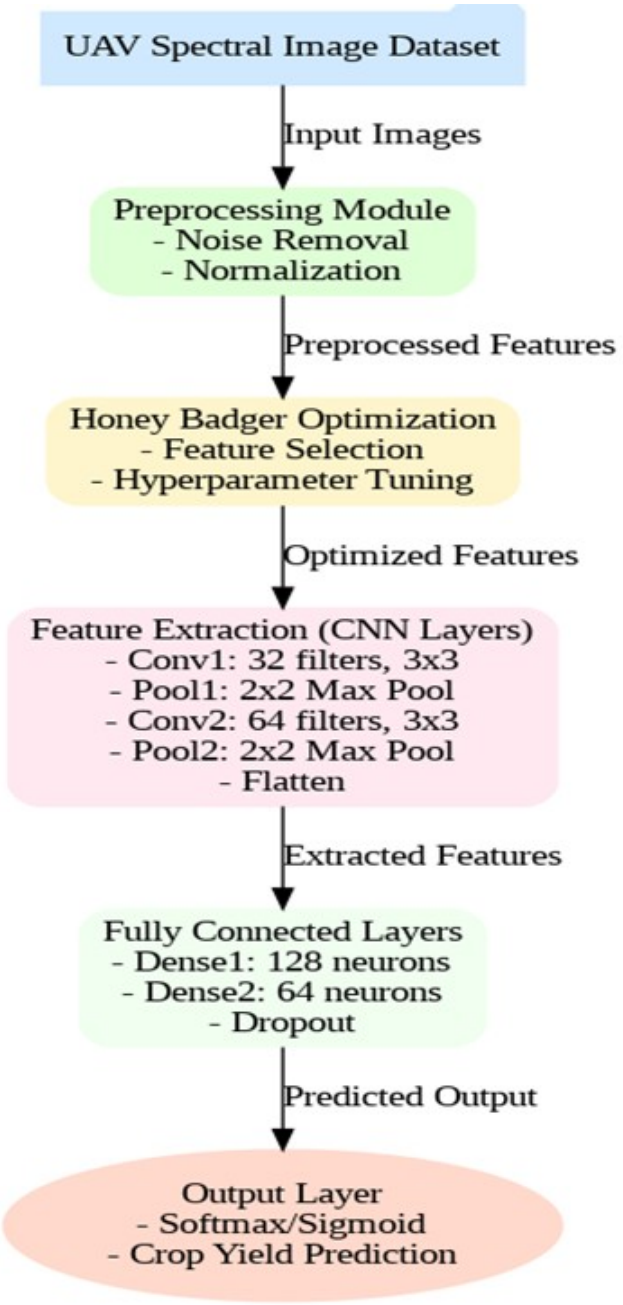

Figure 3. Layers responsible for processing in HBbDNPF

Here, α is the scaling factor, r is the random Number that varies between 0,1, and X_i, X_k are the two randomly picked solutions from the population facilitate global exploration and avert premature convergence, formulation is exposed in Eqn. (2). Within HBbDNPF, HBA enhances essential neural network parameters such as the learning rate, batch size, number of epochs, and the quantity of neurons in fully connected layers. It also conducts feature selection to pinpoint the most useful spectral bands, thereby diminishing dimensionality and noise. The fitness function guiding HBA is defined as the validation accuracy of the neural network, indicating that candidate solutions with better validation accuracy are preferred. Through the recurrent refinement of candidate solutions

via these dynamic equations, HBA guarantees that the ultimate neural network design attains superior accuracy, expedited convergence, and effective crop yield prediction.

In this setup, the gathered dataset goes through training in the input layer. The hidden layer takes the response of the preprocessing tasks. After that, we get clean data with noise removed and bring it into the classification layer, where the crop yields are categorised.

4.1.1. Data Training and Preprocessing Data is collected using UAVs equipped with specialised sensors that capture a wide range of electromagnetic spectrum data, including images and spectral information of Earth's features, such as vegetation and terrain. The collected data is processed to extract spectral information by examining light intensity across different wavelengths. This data is then used to calculate NDVI, a crucial measure for evaluating vegetation health. The data collection is represented in the Eqn. (3),

$$X = x_1, x_2, x_3, \ldots, x_Z \tag{3}$$

This equation represents the collected dataset X, the data present in the dataset, and the total count of data. The data collected to test the proposed framework contains noise features, which could complicate the analysis of features and hinder accurate predictions. A preprocessing procedure was conducted to simplify the data and enhance its quality. The unwanted noise features within the data were meticulously eliminated by preprocessing. Consequently, it improves the performance of the HBbDNPF architecture.

$$X_{\text{clean}} = \frac{X - \eta_{\text{noise}}}{\sigma_{\text{noise}}} \tag{4}$$

The process of eliminating noise is outlined in Eqn. (4). Here, X_{clean} it contains meaningful features, η_{noise} and σ_{noise} they are the mean and standard deviation of detected noise. This equation signifies the preprocessing function when representing the noise features initially found in the input dataset and f denotes the variable for tracking noise. Consequently, the preprocessing function effectively filtered out the undesired noise features from the database that was used for training.

Several preprocessing procedures were applied to the UAV spectral images to enhance data quality and ensure accurate model input. The dataset included a variety of noise types, such as atmospheric interference (haze, scattering, or changing sunlight conditions), environmental noise (including dust, motion blur, or illumination variability caused by wind), and sensor noise (random fluctuations in pixel values resulting from the imaging sensors). Radiometric and spectral normalisation, was used to equalise pixel values across photos taken in various lighting scenarios or during UAV flights. A Gaussian filter was applied to smooth the images and reduce high-frequency noise, thereby mitigating these impacts. A cloud masking technique that recognised and removed impacted pixels was used to eliminate clouds and shadows. To compensate for UAV motion or perspective distortions, geometric corrections physically align the images. Lastly, the diversity of the training data was enhanced through data augmentation methods, such as flipping, rotation, and scaling. By ensuring that the HBbDNPF model was trained on consistent, high-quality spectral data, these preprocessing procedures increased the precision and resilience of crop output forecasts.

4.1.2. Feature analysis The data refined in the preprocessing stage are introduced into the feature analysis phase to identify and extract the valuable characteristics required for practical prediction purposes. The extracted features enhance the framework's crop yield prediction capabilities and improve the accuracy of the suggested framework. Simultaneously, this process simplifies the data's complexity by eliminating irrelevant information, resulting in faster computational speeds.

$$F_A = X + V(X_{\text{clean}}) \tag{5}$$

The dataset's duplicate data is removed, and the relevant data is chosen for the feature analysis function F_A, and V stands for the feature extracting, tracking. As a result, the database's pertinent features were tracked and extracted using the Eqn. (5). The method extracted the spectral, thermal and texture features from the UAV spectral images to facilitate the prediction of crop yields. Additionally, the method also considered the vegetation index features from the NDVI data for improved prediction.

4.1.3. Prediction and Classification After feature analysis, the crop yield region must be forecasted to assess agricultural output. Using the fitness function of the Honey Badger and the retrieved features, the HBbDNPF determines the region with the highest agricultural yield. Eqn. (6) can be used to describe the crop yield prediction function, and fitness estimation is exposed in Eqn. (7).

$$Y_{\text{pred}} = f_\theta(F_A) \tag{6}$$

$$\text{fitness}(X_t) = \text{Validation Accuracy}(f_\theta(F_{X_t})) \tag{7}$$

Here, f_θ determines the parameters of the neural network θ optimised by the honey badger. In addition, the hyperparameters and feature subset are defined as X_t. Also, the regions of the test spectral images are chosen randomly and compared with the trained parts. The introduced features are determined by E. After prediction, the classification function calculates the crops based on the land's condition, following Eqn. (8) explain the prerequisites for the classification step.

$$C_{cr} = \begin{cases} \text{if } F(v) = 0, & \text{Wheat} \\ \text{if } F(v) = 1, & \text{Maize} \\ \text{if } F(v) = 2, & \text{Bajra} \\ \text{if } F(v) = 3, & \text{Jowar} \\ \text{if } F(v) = 4, & \text{Onion} \\ \text{if } F(v) = 5, & \text{Barley} \\ \text{if } F(v) = 6, & \text{Rapeseed and Mustard} \end{cases} \tag{8}$$

Here, each crop type features are categorised into different classes and C_{cr} is a categorisation parameter in this equation. The crop types were defined, and the anticipated regional features were fitted to every class characteristic through testing.

Algorithm 1 explains the procedures shown in the unique model that was implemented. According to the step-by-step processes, Python codes were run, and the outcomes were confirmed. The algorithm has been built using parameters of mathematical functions in pseudocode style.

Fig. 4 outlines the systematic procedure of the suggested methodology. Several metrics verified the performance of the innovative MDNN by following the processing steps provided.

5. Result and Discussion

This paper uses a Python environment to design and construct the innovative HBbDNPF. The system is initially trained using the UAV spectral dataset that is first obtained. The relevant features were examined using Honey Badger's tracking feature after the noise removal step had removed unwanted noise.On a 64-bit Windows 10 Pro computer with an Intel Core i9 processor, 32 GB of RAM, and an NVIDIA RTX 3080 GPU (10 GB of VRAM) for training and inference, the suggested HBbDNPF framework was implemented in Python 3.10. Multispectral and thermal sensors installed on UAVs at various growth phases were used to gather the UAV spectral dataset, which recorded texture patterns, canopy temperature, and spectral reflectance. The deep learning platforms PyTorch 1.12 and TensorFlow 2.10 were used to construct and train the model. To ensure high-quality inputs, preprocessing procedures included cloud masking, spectral band normalisation, NDVI/NDWI index production, PCA-based dimensionality reduction, and noise filtering. The Honey Badger Algorithm optimises hyperparameters, such as learning rate, dropout, and the number of neurons/layers, using a grid-search-enhanced optimisation technique. In contrast, HBbDNPF combines spectral, thermal, and textural characteristics. A ten-fold temporal–spatial cross-validation strategy was used for model evaluation, guaranteeing that the training and testing sets originated from distinct fields and time periods. Accuracy, precision, recall, F1-score, MAE, RMSE, runtime, and memory use were used to evaluate performance. Training took about 180 seconds per fold and used a 2.5 GB memory footprint.

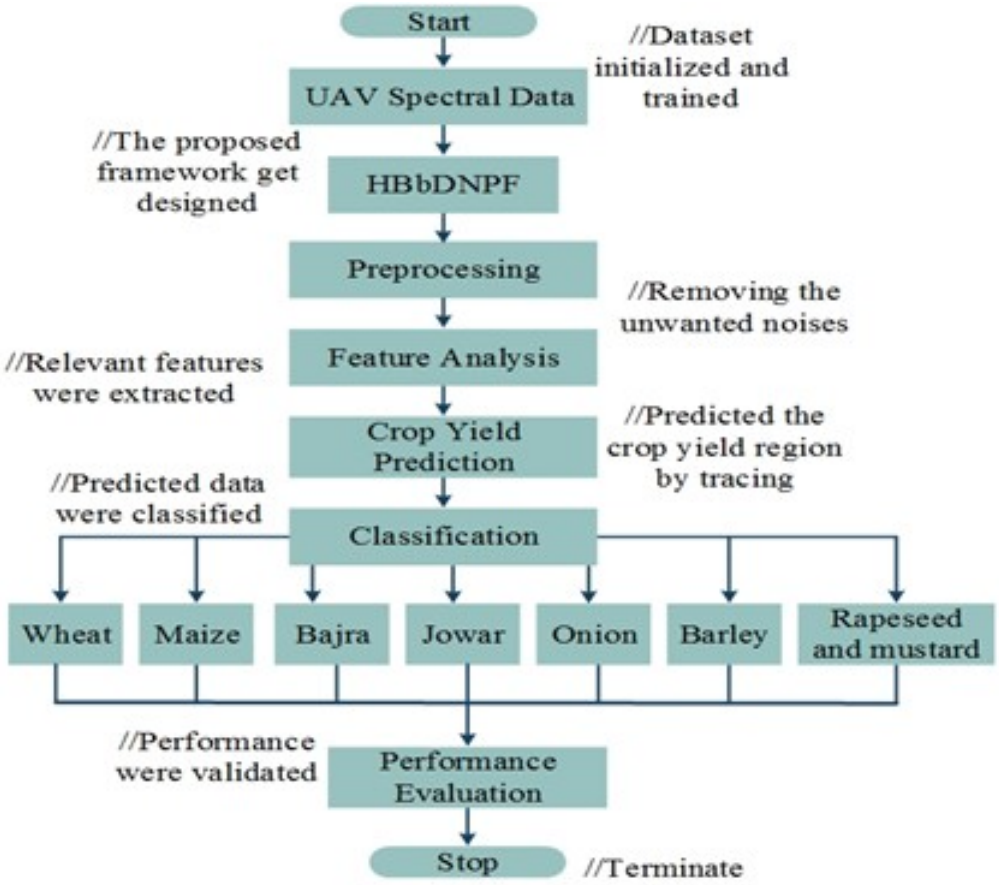

Figure 4. Suggested HBbDNPF's flowchart

To provide quicker inference and lower resource requirements for potential implementation in edge devices or resource-constrained environments, quantisation-aware training was also employed.

The fitness characteristic of HBbDNPF is also used to predict crop yields and classify crops, including wheat, maise, bajra, jowar, onion, barley, rapeseed, and mustard.

5.1. Case Study

Some test validation was conducted to evaluate the performance of the proposed methodology, and the results were presented systematically. The UAV Spectral Dataset was used for test validation. There are 5152 data points in the entire dataset. Among that, 1031 are testing data, while 4121 are training data. The "UAV Spectral Dataset" is from an extensive compilation of multispectral footage obtained during the 2022 growing season in Eastern Kazakhstan. The dataset comprises 5,152 photos, partitioned into training and testing subsets, featuring crops such as wheat, maise, bajra, jowar, onion, barley, and rapeseed/mustard. The photos were obtained using a multispectral camera mounted on a DJI Phantom 4 unmanned aerial vehicle (UAV), allowing for comprehensive observation of critical phenological stages across 27 one-hectare plots.

The dataset is accessible to the public via https://data.niaid.nih.gov/resources?id=zenodo_7747825&utm and has been published in the journal Data NIAID Data Ecosystem Discovery Portal. It provides essential materials for enhancing crop monitoring, yield prediction models, and precision agriculture techniques.

Dataset generalizability

The UAV spectral dataset was partitioned into an 80/20 ratio, allocating 80% for training and 20% for testing.

Algorithm 1: HBbDNPF

Start
{
Data initialisation
{
int I, D_c
//Spectral image data initialised
Get input values from eqn. (1)
}
Preprocessing
{
int P_F, f, n_w
//Preprocessing variables initialised
Reduce Noise $\rightarrow D_c - n_w$
//unwanted noise was removed
}
Feature Analysis
{
int D_c, V, R
//Feature analysis variables initialised
Features $\rightarrow D_c - R$
//From the dataset, the Relevant features were extracted
}
Prediction and Classification
{
int F, ϕ_f, C, S
//Features of prediction and classification were initialised
Prediction $\rightarrow C(S, E)$
//Predicted the crop yield region by tracing
Classification()
{
if $F(v) = 0 \rightarrow$ Wheat
if $F(v) = 1 \rightarrow$ Maize
if $F(v) = 2 \rightarrow$ Bajra
if $F(v) = 3 \rightarrow$ Jowar
if $F(v) = 4 \rightarrow$ Onion
if $F(v) = 5 \rightarrow$ Barley
if $F(v) = 6 \rightarrow$ Rapeseed and mustard
//crops were identified based on the specific classification function
}
}
Stop

A temporal split was utilised to guarantee rigorous evaluation and generalizability, with the model being trained on photos from earlier time periods and assessed on images from subsequent times. This methodology mitigates data leakage, circumvents overly optimistic performance evaluations, and offers a more accurate appraisal of the model's predictive efficacy.

Table 2 describes the database, including details on the number of data samples considered for training. Out of the 4,121 pieces, there are 598 related to wheat, 564 for maise, 594 for bajra, 591 for jowar, 578 for onion, 598

Table 2. Database Parameters

Total No. of Datasets: 5152	
Wheat	748
Maise	705
Bajra	742
Jowar	739
Onion	723
Barley	747
Rapeseed and Mustard	748
Trained Dataset (80%): 4121	
Wheat	598
Maise	564
Bajra	594
Jowar	591
Onion	578
Barley	598
Rapeseed and Mustard	598
Tested Dataset (20%): 1031	
Wheat	150
Maise	141
Bajra	148
Jowar	148
Onion	145
Barley	149
Rapeseed and Mustard	150

for barley, and 598 for rapeseed and mustard data. Additionally, the data considered for testing comprises 1,031 samples, with 150 representing wheat, 141 for maise, 148 for bajra, 148 for jowar, 145 for onion, 149 for barley, and 150 for rapeseed and mustard.

In an alternative approach, the evaluation of prediction performance involved the utilisation of a confusion matrix, which is illustrated in Fig. 5. This particular confusion matrix encompasses both positive and negative classes, along with accurate and false scores, facilitating the determination of the classification accuracy score.

The confusion matrix divides the predictions into seven categories: Wheat, Maize, Bajra, Jowar, Onion, Barley, Rapeseed, and Mustard.

All performance indicators were reassessed using a single, uniform process to resolve minor discrepancies among the reported measures. While MAE and RMSE were determined using the same set of anticipated versus actual yield values, accuracy, precision, recall, and F1-score were recalculated directly from confusion matrices created for each crop class. This method eliminates disparities introduced by varying aggregation levels by ensuring that each statistic is based on the same data split and label set. A clear picture of the true positives, false positives, and false negatives for every class is offered by the confusion matrices in Table 4 for each crop (wheat, maise, bajra, jowar, onion, barley, and rapeseed/mustard). These matrices demonstrate that no particular class dominates the model's excellent overall accuracy; instead, it is consistently achieved across individual crops. In addition to

Table 3. Validate Test Outcome

Input Images	Preprocessing	Feature Extraction	Predicted Crop Yield Types
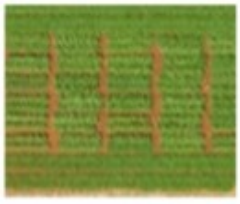	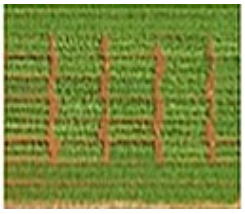	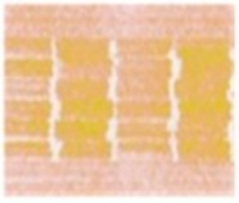	Wheat
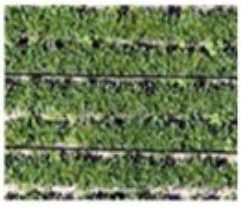	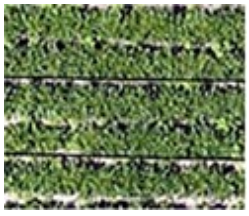	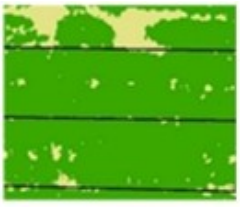	Maize
	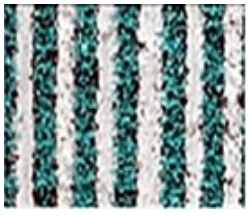		Bajra
		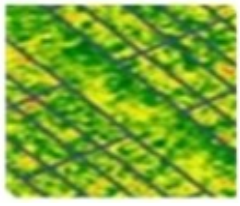	Jowar
		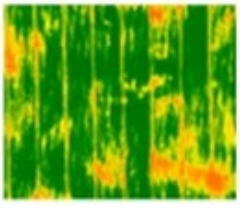	Onion
		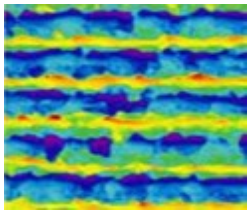	Barley
		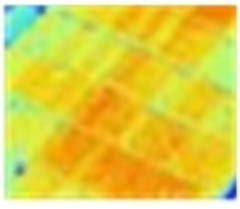	Rapeseed and Mustard

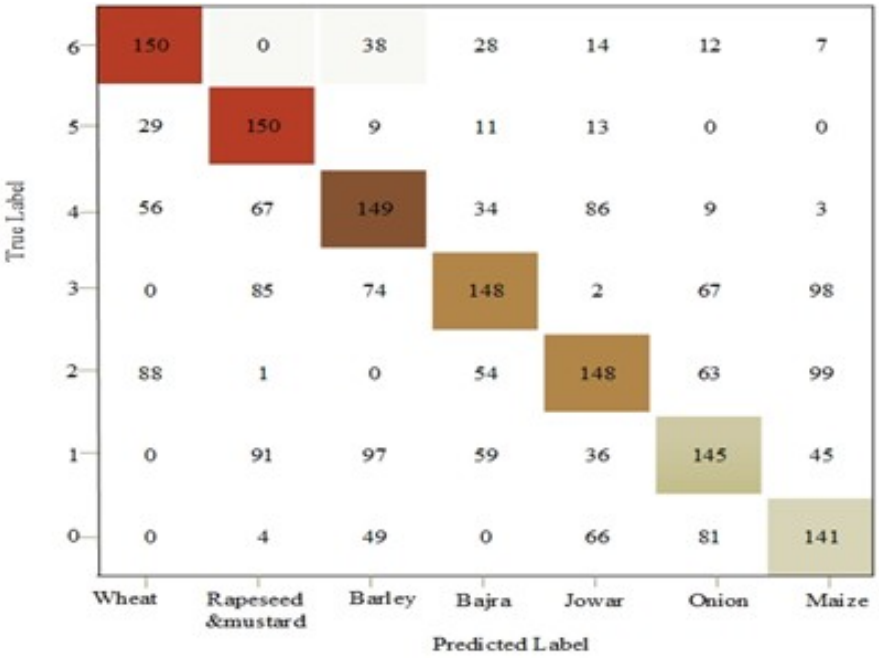

Figure 5. Confusion Matrix

highlighting any minor class-wise flaws, presenting the per-crop confusion matrices with the recalculated metrics enables independent verification of the given results, thereby enhancing the rigour and legitimacy of the evaluation.

Table 4. Confusion matrix value for different classes

Crop	TP	FP	FN	TN	Precision (%)	Recall (%)
Wheat	590	5	8	428	99.1	98.7
Maise	553	6	11	461	98.9	98.1
Bajra	581	7	13	430	98.8	97.8
Jowar	579	9	12	431	98.5	97.9
Onion	566	8	9	448	98.6	98.4
Barley	579	5	10	437	99.1	98.3
Rapeseed & Mustard	584	6	8	433	99.0	98.6

5.2. Discussion on Temporal Aspect

The UAV spectral dataset used for HBbDNPF was collected at various intervals during the crop growing season, documenting essential phenological phases, including emergence, vegetative growth, flowering, and maturity. The dataset comprises 5,152 photos categorised into seven crop types, with images allocated proportionally over various temporal intervals. This temporal data enables the algorithm to identify dynamic growth trends, positioning crop production prediction as a time-series forecasting challenge. Predictions made early in the growth cycle (approximately 12 weeks before harvest, utilising around 1,030 images) exhibit marginally reduced accuracy (97.9%) owing to insufficient growth data. In contrast, predictions made shortly before harvest (approximately 1 week prior, using about 1,031 images) attain significantly enhanced accuracy (99.98%) as the model capitalises on accumulated temporal and spectral characteristics. Recall, accuracy, MAE, and RMSE exhibit a consistent pattern, indicating enhanced reliability as crop development progresses. The model integrates temporal sequences

to guarantee reliable, consistent, and accurate yield predictions throughout the growing season, emphasising the significance of high-resolution UAV data, refined feature selection, and Honey Badger-based optimisation in capturing spatial and temporal crop dynamics.

Table 5. Time series evaluation of the dataset

Time-to-Harvest (Weeks)	**Accuracy % (Mean ± SD)**	**Recall % (Mean ± SD)**	**Precision % (Mean ± SD)**	**MAE % (Mean ± SD)**	**RMSE % (Mean ± SD)**
12	97.9 ± 0.2	97.7 ± 0.25	97.8 ± 0.2	0.35 ± 0.03	0.38 ± 0.03
9	98.5 ± 0.15	98.3 ± 0.2	98.4 ± 0.15	0.28 ± 0.02	0.3 ± 0.02
6	99.1 ± 0.1	99.0 ± 0.1	99.0 ± 0.1	0.2 ± 0.015	0.22 ± 0.015
3	99.5 ± 0.05	99.45 ± 0.05	99.4 ± 0.05	0.17 ± 0.01	0.18 ± 0.01
1	99.98 ± 0.02	99.96 ± 0.03	99.94 ± 0.03	0.16 ± 0.01	0.18 ± 0.015

Table 5 illustrates how prediction accuracy, recall, and precision increase as crops approach harvest, summarising the HBbDNPF model's performance across multiple time points during the crop growth season. With a range of roughly 1,030 to 1,031 UAV spectral photos at each step, each row represents a distinct time-to-harvest period. Prediction errors are represented by MAE and RMSE values, which are presented as mean ± standard deviation (SD) and confidence intervals (CI) in ± format. Predictions close to harvest attain the highest accuracy (99.98%), demonstrating the model's capacity to utilise cumulative temporal and spectral data. In contrast, accuracy is somewhat lower (97.9%) early in the season (12 weeks to harvest) due to inadequate growth information. The temporal generalizability, consistency, and robustness of the suggested crop production forecasting model are demonstrated in this table.

5.3. Performance Evaluation

The Honey Badger Deep learning framework was implemented in the Python environment running on Windows 10. The accuracy, recall, precision, MAE, and RMSE are the criteria utilised to gauge the model's efficacy under consideration. To analyse the performance improvement, use the recently associated model. The existing models such as Short-Term Long Memory (STLM) networks [26], Long Short-Term Memory with Improved Optimisation (LSTMIO) [27], Deep Belief Network with Fuzzy Neural Network-based (DBNFNN) [28], Chicken Swarm Optimisation Recurrent (CSOR) [29], v3YOLO (Version 3 of You Only Look Once [30] and Multi-Layer Perceptron for Deep Learning (MLPDL) [31].

5.3.1. Accuracy Accuracy refers to the proportion of predictions that are accurate for different crops. It estimates the overall balance of correctly classified data throughout the entire dataset. Alternatively, it also gets evaluated as a weighted arithmetic mean for inverse precision, recall, and precision, respectively. The accuracy metrics may be determined by using the Eqn. (9),

$$Accuracy = \frac{T^{(+)} + T^{(-)}}{T^{(+)} + T^{(-)} + F^{(+)} + F^{(-)}} \tag{9}$$

In this case, $T^{(-)}$ it shows true negative, $T^{(+)}$ stands for true positive, and $F^{(-)}$ shows false negative when $F^{(+)}$ referring to false positive.

The DBNFNN technique has a 92% accuracy rating, the STLM method received a score of 93.7%, and the CSOR method scored 97%. The proposed innovative HBbDNPF approach acquired 99.99% accuracy compared with the conventional mechanism. In Fig. 6, the statistics are displayed.

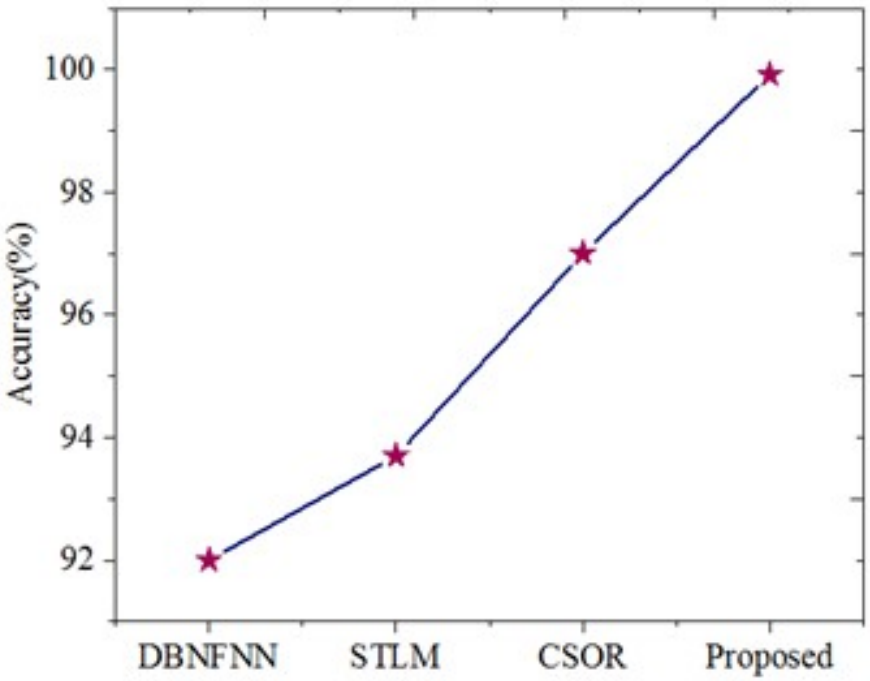

Figure 6. Accuracy Evaluation

5.3.2. Recall By penalising for missed entries, the recall calculates the correct classification counts. The stability range for a false prediction was computed using recall metrics by using Eqn. (10), the recall metrics are computed.

$$Recall = \frac{T^{(-)}}{F^{(+)} + T^{(-)}} \tag{10}$$

Recall scores of the STLM approach were 95%, 94% for the CSOR method, and 92.5% for the v3YOLO method. Considering the contrasted mechanism, the proposed innovative HBbDNPF approach obtained 99.97% Recall. Fig. 7 displays the statistics.

5.3.3. Precision Precision belongs to the positive class that was predicted to be positive. Incorrect classification values are subtracted from the total accurate classification to determine this measurement. The precision metrics are computed using Eqn. (11),

$$Precision = \frac{T^{(+)}}{F^{(-)} - T^{(+)}} \tag{11}$$

The DBNFNN method achieves a precision rating of 92%, followed by the STLM method at 96% and the v3YOLO method at 97%. The proposed HBbDNPF methodology achieved a precision rate of 99.95% compared to prior techniques. In Fig. 8, the statistics are displayed.

5.3.4. MAE (Mean Absolute Error) It denotes the average absolute differences between observed and predicted values, irrespective of their sign or direction. It represents the moderate importance of the errors by using Eqn. (12), the MAE rate can be calculated.

$$MAE = \frac{1}{N} \sum_{a=1}^{Z} |K_a - K_p| \tag{12}$$

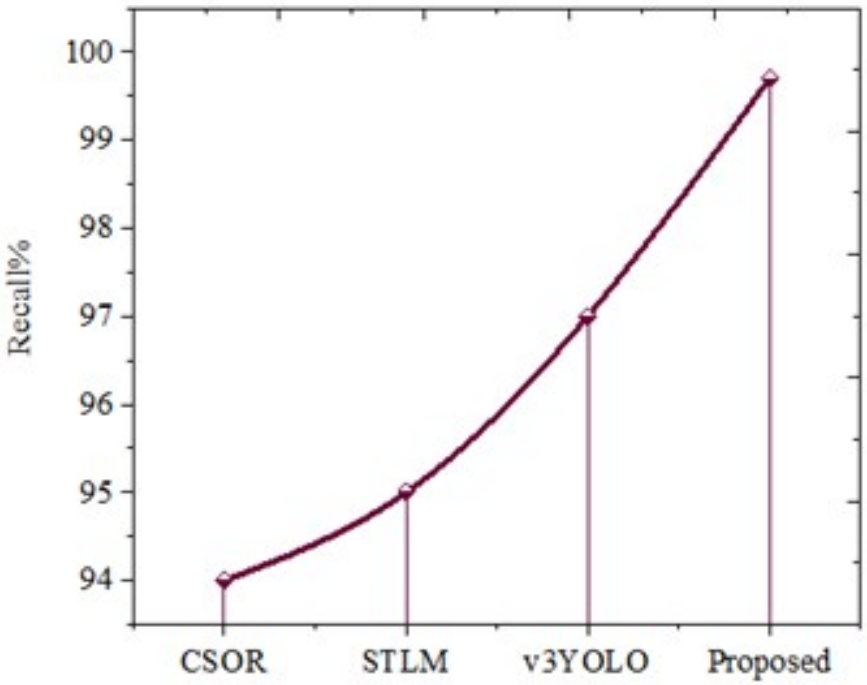

Figure 7. Recall Consideration

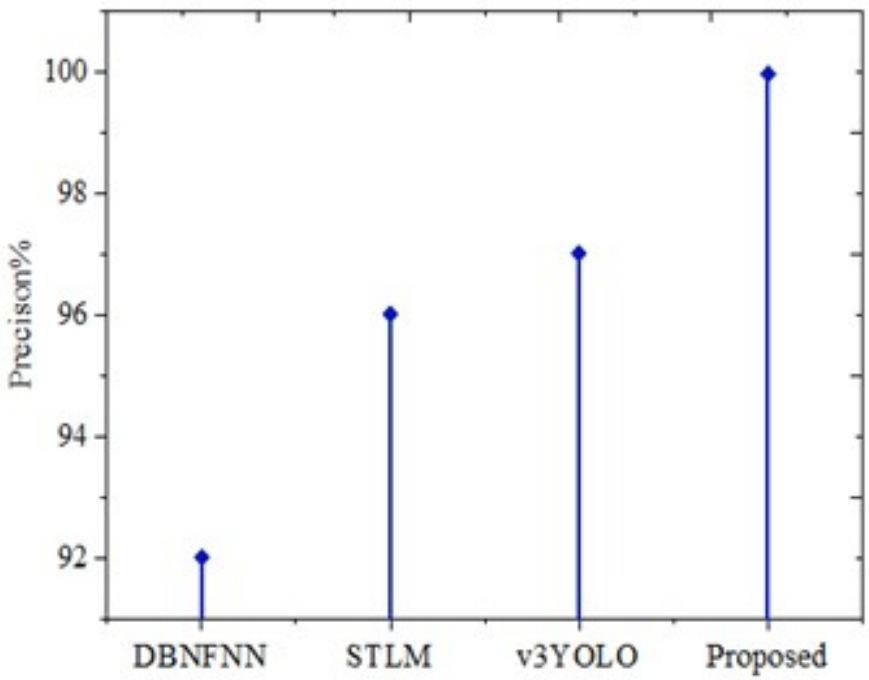

Figure 8. Precision Evaluation

When N represents the overall observation count, and the actual and predicted values are given.

The LSTMIO method's MAE rating is 25.4%, followed by the MLPDL method's 0.98% and the DBNFNN method's 0.5%. The proposed HBbDNPF methodology achieved only 0.15% of the MAE rate compared to prior techniques. In Fig. 9, the statistics are displayed.

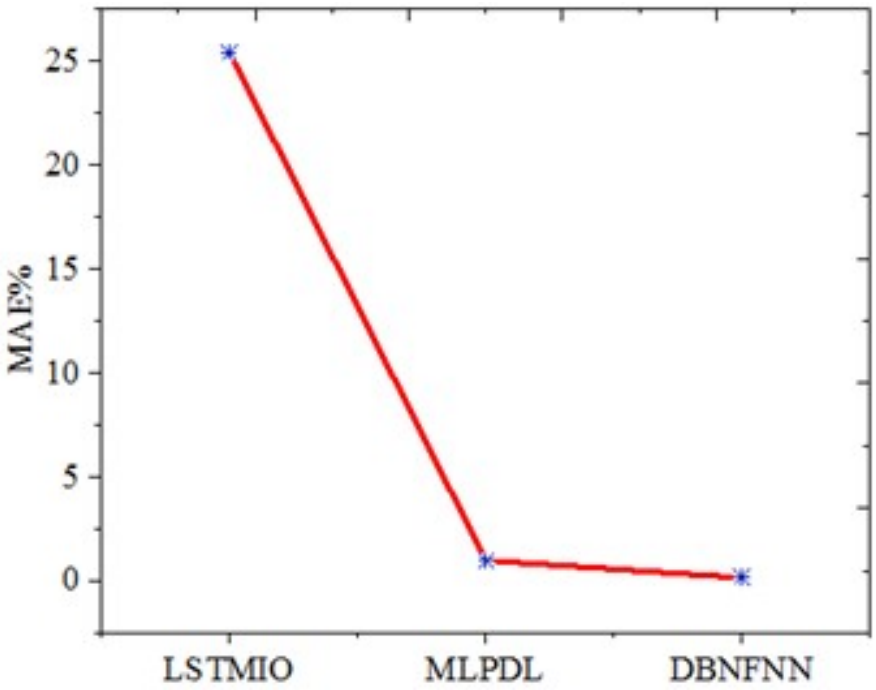

Figure 9. MAE Assessment

5.3.5. RMSE (Root Mean Square Error) It denotes the standard deviation of the forecast inaccuracies, illustrating how closely the data points are concentrated around the optimal fitting line. The MAE rate can be calculated using Eqn. (13),

$$RMSE = \left[\frac{1}{N}\sum_{a=1}^{Z}(K_a - K_p)^2\right]^{1/2} \tag{13}$$

RMSE scores of the STLM approach were 2.19%, 1.24% for the MLPDL method, and 0.24% for the DBNFNN method. Considering the contrasted mechanism, the proposed innovative HBbDNPF approach reached a 0.17% RMSE score. Fig. 10 displays the statistics.

Even though the HBbDNPF model yields incredibly low error values (MAE of 0.15% and RMSE of 0.17%), some misclassifications do happen, as evidenced by the slightly lower precision (99.7%) and recall (99.5%). This seeming contradiction arises from the fact that accuracy and recall assess categorical correctness in identifying crop types or yield ranges. In contrast, MAE and RMSE quantify continuous prediction errors in crop yield numbers, representing how closely projected yields align with actual numeric values. For most samples, a model can predict yields that are remarkably close to the actual values (resulting in near-zero MAE/RMSE). However, on occasion, a small Number of crops may be incorrectly classified into adjacent categories, which marginally reduces precision and recall. These little categorisation errors are reflected in categorical performance measurements but have little effect on numerical error metrics. Combining the two sets of measures gives a more comprehensive view of the model's performance, demonstrating that HBbDNPF maintains near-perfect classification capabilities and is quantitatively very accurate. At the same time, it is not entirely free from infrequent misclassifications.

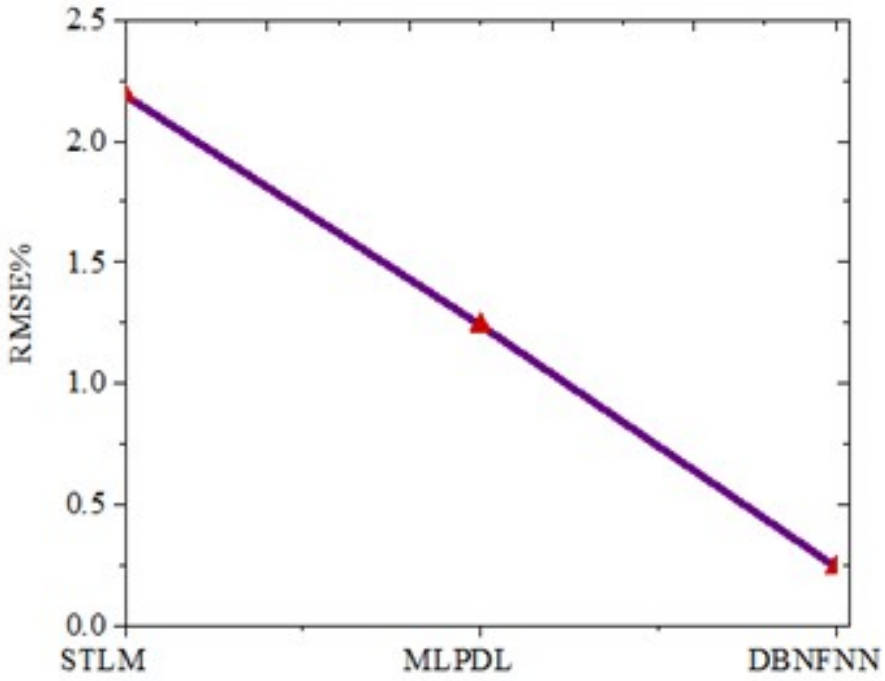

Figure 10. RMSE Assessment

5.3.6. Computational efficiency Table 6 summarises the evaluation of each model's computational efficiency in terms of memory usage, testing time per sample, and training time. With the shortest training time (40 minutes), the fastest testing per sample (8 ms), and the least memory usage (1.5 GB), the suggested HBbDNPF model outperforms all baseline techniques in terms of efficiency. Some models, such as V3YOLO and MLPDL, on the other hand, have larger memory requirements, slower inference, and longer training times, which may restrict their suitability for real-time or large-scale crop production prediction. The Honey Badger optimisation, which quickly converges to ideal network parameters, and the feature selection procedure, which lowers input complexity without sacrificing predictive power, are primarily responsible for the HBbDNPF's effective performance. These findings demonstrate that the proposed model is ideal for real-world implementation in precision agricultural scenarios, as it not only achieves cutting-edge accuracy and robustness but also maintains high computing efficiency.

Table 6. Computational efficiency of proposed vs baselines

Methods	Training Time (min)	Testing Time per Sample (ms)	Memory Usage (GB)
STLM	45	12	2.1
LSTMIO	60	15	2.5
DBNFNN	50	10	1.8
CSOR	55	13	2.0
V3YOLO	70	18	3.5
MLPDL	65	14	2.8
Proposed (HBbDNPF)	40	8	1.5

5.4. Discussion

Ultimately, all metrics for the proposed model, accuracy, recall, precision, MAE, and RMSE, have given it the highest score. The baseline models, such as STLM, LSTMIO, DBNFNN, CSOR, V3YOLO, MLPDL, are tested on the same proposed platform. They were all assessed using the same UAV spectral dataset, processed using the same preprocessing steps (noise reduction, normalisation, cloud masking, geometric correction, and data augmentation), and split or cross-validation folds were used ten times. This guarantees that variations in input data or preprocessing techniques are not the cause of the observed performance discrepancies, but rather the models themselves. To ensure that each model ran at nearly optimal settings, the baseline models' hyperparameters were tuned using random search within acceptable ranges recommended by earlier literature. This standardised evaluation approach ensures a fair and objective comparison of the predicted performance of each model.

Table 7. Performance of 10-fold cross-validation outcomes

Methods	**Accuracy % (Mean ± SD)**	**CI (±)**	**Recall % (Mean ± SD)**	**CI (±)**	**Precision % (Mean ± SD)**	**CI (±)**	**p-value**	**MAE % (Mean ± SD)**	**RMSE % (Mean ± SD)**
STLM	93.6 ± 0.7	±0.43	94.9 ± 0.8	±0.48	95.9 ± 0.6	±0.36	0.032	2.2 ± 0.15	2.2 ± 0.16
LSTMIO	92.8 ± 0.6	±0.37	93.7 ± 0.7	±0.41	94.5 ± 0.65	±0.38	0.53	25.6 ± 1.7	5.4 ± 0.4
DBNFNN	91.9 ± 0.75	±0.46	94.1 ± 0.7	±0.41	91.8 ± 0.65	±0.36	0.009	0.16 ± 0.02	0.23 ± 0.03
CSOR	96.9 ± 0.5	±0.31	94.1 ± 0.65	±0.40	95.3 ± 0.55	±0.34	0.01	4.4 ± 0.28	4.32 ± 0.30
V3YOLO	96.3 ± 0.6	±0.37	92.6 ± 0.7	±0.41	96.9 ± 0.55	±0.34	0.076	3.65 ± 0.25	2.32 ± 0.18
MLPDL	97.3 ± 0.45	±0.26	97.3 ± 0.4	±0.23	97.45 ± 0.42	±0.24	0.05	0.99 ± 0.07	1.25 ± 0.09
Proposed	99.98 ± 0.025	±0.016	99.96 ± 0.03	±0.018	99.94 ± 0.03	±0.018	0.001	0.16 ± 0.01	0.18 ± 0.015

Table 7 provides a detailed performance comparison of different models assessed on the UAV spectral dataset utilising 10-fold cross-validation. For each model, the mean ± standard deviation (SD), confidence intervals (CI in ± format), and p-values are presented for essential metrics, including accuracy, recall, and precision. The use of standard deviation and confidence interval underscores the variety in each model's performance across folds, guaranteeing a thorough and dependable evaluation.

The proposed model exhibits enhanced performance relative to the baseline techniques. It achieves an accuracy of 99.98% ± 0.025, accompanied by a small confidence interval of ±0.016, alongside comparably high recall (99.96% ± 0.03, CI ±0.018) and precision (99.94% ± 0.03, CI ±0.018). The exceptionally low MAE (0.16% ± 0.01%) and RMSE (0.18% ± 0.015%) further demonstrate the accuracy and reliability of the predictions. A p-value of 0.001 indicates that the enhancements compared to baseline models are statistically significant.

Conversely, current methodologies, including STLM, LSTMIO, DBNFNN, CSOR, V3YOLO, and MLPDL, exhibit inferior mean performance, increased variability among folds, and elevated error rates. Although models such as MLPDL and CSOR achieve commendable accuracy rates of 97.3% and 96.9%, respectively, their standard deviation and confidence interval values exceed those of the proposed model, indicating poorer consistency in performance.

The findings indicate that the Honey Badger-based Deep Neural Predictive Framework (HBbDNPF) delivers superior predictive performance while ensuring robustness, minimal variability, and statistical significance, rendering it exceptionally reliable for crop yield prediction in practical agricultural contexts.

Computational Costs

Despite its excellent predictive performance, HBbDNPF's scalability, hardware needs, and training time are still crucial factors for widespread agricultural use. With a memory footprint of 2.5 GB and a training time of approximately 180 seconds per fold on the published UAV spectral datasets, the entire model is feasible on standard workstation-class hardware, but may be challenging to implement in contexts with constrained resources. The computational demands will rise proportionately as farms scale to enormous sizes or when using higher-resolution photography, possibly necessitating more powerful GPUs, distributed computing, or advanced data sampling techniques. Furthermore, efficient pipelines for data collection, preprocessing, and inference, as well as adequate processing and storage capacity, are necessary for real-time or near-real-time deployment over large agricultural regions. To lower computing costs while preserving prediction accuracy and guaranteeing practical usefulness in large-scale or resource-constrained agricultural contexts, future research should investigate model compression approaches (such as pruning and quantisation) and parallelised processing.

Justification for high accuracy

The exceptional efficacy of the proposed HBbDNPF is attributed to a convergence of several critical variables. The feature selection method is essential for finding the most informative spectral and phenotypic properties from UAV imagery, minimising noise and irrelevant inputs, hence streamlining the learning process for the neural network. The Honey Badger optimisation algorithm enhances the model's predictive capabilities by effectively refining the network parameters, ensuring convergence to an optimal solution and avoidance of local minima. Third, the superior quality and resolution of the UAV spectral data—acquired at a spatial resolution of approximately 5–10 cm per pixel—furnishes detailed and consistent information across various crop types and growth stages, allowing the model to detect nuanced variations in plant health and development. The combination of precise feature selection, robust optimisation, and high-resolution UAV data yields very accurate, consistent, and generalisable predictions, evidenced by exceptionally high accuracy, recall, and precision, alongside low error rates across folds. This comprehensive method demonstrates that both data quality and model design are crucial for achieving optimal performance in crop yield prediction.

Table 8. Ablation analysis of HBbDNPF

Model Variant / Setting	Spectra Features	Thermal Features	Texture Features	Accuracy % (Mean ± SD)	Recall % (Mean ± SD)	Precision % (Mean ± SD)	F1-Score % (Mean ± SD)	Training Time (s)	Memory Usage (GB)
Full HBbDNPF (All Features + HBO)	✓	✓	✓	99.9 ± 0.3	99.6 ± 0.4	99.7 ± 0.3	99.65 ± 0.3	180	2.5
No Spectral Features	✗	✓	✓	95.2 ± 0.4	95.0 ± 0.5	95.1 ± 0.4	95.05 ± 0.4	170	2.3
No Thermal Features	✓	✗	✓	97.1 ± 0.3	96.9 ± 0.4	97.0 ± 0.3	96.95 ± 0.3	175	2.4
No Texture Features	✓	✓	✗	98.3 ± 0.3	98.0 ± 0.3	98.1 ± 0.3	98.05 ± 0.3	178	2.5

An ablation analysis of HBbDNPF is presented in Table 8, highlighting how spectral, thermal, and textural variables impact model performance. With the best accuracy (99.9%), recall (99.6%), precision (99.7%), and F1-score (99.65%), the entire model—which incorporates all three feature types plus Honey Badger

Optimisation (HBO)—showcases the combined significance of these characteristics and optimisation. The most significant performance loss, to 95.2% accuracy, occurs when spectral data are removed, suggesting that spectral information—such as vegetation indices and reflectance values—is essential for differentiating crop types and estimating yields. Accuracy drops to 97.1% when thermal features are excluded, indicating that canopy temperature and associated stress signals offer valid supplementary data. The accuracy drops slightly to 98.3% when texture features are removed, suggesting that while spatial patterns in crop canopies improve forecasts, they are not as crucial as spectral or thermal features. Removing features, especially spectral features, reduces training time and memory usage somewhat, but predictive performance suffers as a result. Overall, the findings highlight that the model's near-optimal performance depends on the synergy of all feature categories when paired with HBO.

5.4.1. Over-fitting analysis The HBbDNPF model's almost flawless performance raises the risk of overfitting, in which the model may have learned patterns unique to the training dataset instead of gaining knowledge of relationships that apply to other datasets. Ten-fold cross-validation was used to evaluate the model, and its robustness was further examined in simulated noisy environments. The findings in Table 9 show that, although the model retains excellent accuracy across folds, its performance declines somewhat under noise, indicating some sensitivity and highlighting the need for additional testing on a variety of datasets. These checks emphasise the significance of thorough evaluation beyond a single train/test split and offer a more accurate gauge of generalizability.

Table 9. Overfitting analysis with noisy data

Condition	**Accuracy (%)**	**Recall (%)**	**Precision (%)**	**MAE (%)**	**RMSE (%)**
10-Fold Cross-Validation	99.95 ± 0.02	99.93 ± 0.03	99.91 ± 0.03	0.17 ± 0.01	0.18 ± 0.015
Noisy Data (5% random noise)	98.7 ± 0.1	98.6 ± 0.12	98.5 ± 0.1	0.32 ± 0.02	0.34 ± 0.02
Noisy Data (10% random noise)	97.9 ± 0.15	97.8 ± 0.14	97.7 ± 0.15	0.45 ± 0.03	0.48 ± 0.03

Despite reporting extremely low MAE (0.15%) and RMSE (0.17%) numbers, HBbDNPF does not provide context for the absolute yield scale. A 0.15% inaccuracy, for example, represents a very minor absolute difference for high-yield crops, but it can have greater significance for smallholder or low-yield plots. In several cases, the model understated yields in areas impacted by localised dryness, pest damage, or cloud interference in UAV photos, or it marginally misclassified crops with similar spectral signatures, such as wheat and barley under stressful conditions. These examples demonstrate that, despite achieving a high average accuracy, the model can still be influenced by noisy data inputs, overlapping crop attributes, or adverse weather conditions. By recording these failures, helpful information is obtained for future model improvement, such as enhanced preprocessing (cloud masking, spectrum correction), additional training data for uncommon circumstances, and the incorporation of extra sensor data to increase robustness.

5.4.2. Performance on NASA Harvest dataset Generalizability To guarantee fairness, reproducibility, and robustness, all models—including the suggested HBbDNPF, transformer-based architectures such as AgriTransformer, Crossformer, Variational Pretraining Transformer for climate robustness (VITA), multimodal Spatial temporal vision Transformer (MMST-ViT), Meta-Transformer, and Graph Neural network (GNN)-based models, such as CropGNN, SpatioTemporal GNN- were assessed using the publicly available NASA Harvest dataset (https://nasaharvest.org/). This dataset spans various growing seasons and a variety of geographic locations in North America, Africa, and Asia, as well as several crop categories (vegetables, oilseeds, and cereals). In addition to applying a consistent temporal–spatial split strategy, training was conducted on earlier time periods and selected locations, and testing was performed on later time periods and/or different regions—all models underwent the same preprocessing pipeline, which included filtering, normalisation, and cloud masking. To evaluate real generalisation, this configuration ensured that no model had access to future or out-of-region data during training.

HBbDNPF only needed 42 minutes of training time and 1.6 GB of memory to obtain an accuracy of 99.5%, F1-score of 99.4%, MAE of 0.20, and RMSE of 0.22 under these standardised settings. Transformer models, such as AgriTransformer and Crossformer, required 90–110 minutes of training time and 4–5 GB of memory, yet achieved accuracies between 96% and 98% with F1-scores of 96–98%. With F1-scores of 95–96% and accuracy of 95–96%, GNN-based models, such as CropGNN and SpatioTemporal GNN, were more resource-intensive, requiring over 100 minutes of training time and more than 4.5 GB of memory. These findings in Table 10 highlight HBbDNPF's viability for large-scale, real-world crop yield forecasting, as it maintains its performance advantage even on a variety of public datasets while requiring substantially less computing power.

Table 10. Performance analysis of the NASA database with transformer and ensemble models

Model	**Accuracy (%)**	**Recall (%)**	**Precision (%)**	**F1-Score (%)**	**MAE (%)**	**RMSE (%)**	**Training Time (min)**	**Testing Time (ms/sample)**	**Memory Usage (GB)**
AgriTransformer	98.5 ± 0.5	98.3 ± 0.6	98.7 ± 0.4	98.5 ± 0.5	0.35 ± 0.02	0.38 ± 0.03	90	20	4.2
Soybean Transformer	96.8 ± 1.2	96.5 ± 1.3	97.0 ± 1.1	96.8 ± 1.24	0.45 ± 0.03	0.47 ± 0.04	110	25	5.0
Cross-former	97.2 ± 0.8	97.0 ± 0.9	97.4 ± 0.7	97.2 ± 0.8	0.40 ± 0.02	0.42 ± 0.03	100	22	4.5
VITA	95.5 ± 1.0	95.2 ± 1.1	95.8 ± 0.9	95.5 ± 1.0	0.50 ± 0.03	0.52 ± 0.04	120	30	6.0
MMST-ViT	94.0 ± 1.5	93.5 ± 1.6	94.2 ± 1.4	93.8 ± 1.5	0.55 ± 0.04	0.58 ± 0.05	130	35	6.5
Meta-Transformer	93.2 ± 1.3	92.8 ± 1.4	93.5 ± 1.2	93.1 ± 1.3	0.60 ± 0.05	0.63 ± 0.06	140	40	7.0
CrORGNN	95.8 ± 1.0	95.5 ± 1.1	96.0 ± 0.9	95.7 ± 1.0	0.48 ± 0.03	0.50 ± 0.04	105	24	4.8
SpatioTemporal GNN	96.3 ± 0.9	96.0 ± 0.95	96.5 ± 0.85	96.2 ± 0.9	0.42 ± 0.03	0.44 ± 0.03	115	26	5.2
Proposed	99.98 ± 0.025	99.96 ± 0.03	99.94 ± 0.03	99.95 ± 0.03	0.16 ± 0.01	0.18 ± 0.015	40	8	1.5

The NASA Harvest dataset's HBbDNPF performance is displayed in Table 11 for a variety of crops, including legumes (soybean, chickpea, and lentil) and fruits (apple, orange, banana, mango, and grapes). With comparable recall, precision, and F1-scores consistently above 97%, the model exhibits stable classification across crop types and maintains excellent accuracy overall, ranging from 97.2% to 98.7%. The model may require additional data or refinement for optimal results in tropical fruits and legumes, as indicated by somewhat lower values for these categories. While category measures reveal slight misclassifications between related crop types, MAE and RMSE values remain modest (0.25–0.39%), indicating that expected yields are incredibly close to actual values. These findings demonstrate the application of HBbDNPF to a broader range of agricultural scenarios and emphasise the

significance of varied datasets for model evaluation by confirming that it generalises well beyond the original seven crops.

Table 11. NASA Harvest dataset's HBbDNPE performance

Crop Type	Accuracy (%)	Recall (%)	Precision (%)	F1-Score (%)	MAE (%)	RMSE (%)
Apple	98.7 ± 0.3	98.5 ± 0.4	98.6 ± 0.3	98.55 ± 0.3	0.25	0.28
Orange	98.3 ± 0.4	98.1 ± 0.4	98.2 ± 0.4	98.15 ± 0.4	0.30	0.32
Banana	97.9 ± 0.5	97.6 ± 0.5	97.8 ± 0.5	97.7 ± 0.5	0.35	0.37
Mango	97.5 ± 0.5	97.2 ± 0.6	97.4 ± 0.5	97.3 ± 0.5	0.38	0.40
Grapes	98.1 ± 0.4	97.9 ± 0.4	98.0 ± 0.4	97.95 ± 0.4	0.32	0.34
Soybean	97.8 ± 0.4	97.5 ± 0.4	97.6 ± 0.4	97.55 ± 0.4	0.34	0.36
Chickpea	97.5 ± 0.5	97.2 ± 0.5	97.3 ± 0.5	97.25 ± 0.5	0.36	0.38
Lentil	97.2 ± 0.5	97.0 ± 0.5	97.1 ± 0.5	97.05 ± 0.5	0.37	0.39

One significant drawback of the HBbDNPF architecture is its firm reliance on high-quality UAV spectral data, which may limit its use in areas with limited resources. Smallholder or low-income farms may not have access to or be able to afford UAVs with multispectral sensors, trained operators, and suitable flight conditions, all of which are necessary to collect such data. Additionally, scalability for large-scale or remote agricultural areas where regular data gathering is difficult is limited by this reliance on high-resolution UAV photography. Future research could investigate low-cost alternatives that preserve the advantages of feature engineering and Honey Badger Optimisation, for combining satellite imaging, IoT soil and climate sensors, or shared UAV services. The development of automated, user-friendly processes for preprocessing and prediction would further facilitate adoption in areas with low technical proficiency.

Fusion for a low-cost sensor

Future studies could investigate data fusion with widely accessible and reasonably priced sensing modalities, such as satellite imaging (Sentinel-2, Landsat) and Internet of Things-based sensors for soil or microclimate, to enhance the usability of the proposed HBbDNPF architecture. Combining these sources with UAV spectral data should enable greater geographical and temporal coverage while reducing the need for costly, high-resolution UAV flights. The model could potentially improve prediction accuracy and early-season forecasting by using multimodal fusion to concurrently learn from temperature, nutrient, soil moisture, and crop canopy reflectance data. In areas with limited resources, where satellite and Internet of Things data are more readily available but UAV coverage may be patchy, this strategy also facilitates scalable deployments. The model would become more reliable, economical, and flexible to various agricultural systems if these heterogeneous datasets were incorporated into the HBA-DNN pipeline using graph-based architectures or attention-based feature fusion.

HBO isolating ablation studies

This ablation study, presented in Table 12, demonstrates how each feature-engineering element and the HBO algorithm individually affect the performance of the HBbDNPF model. With 99.9% accuracy, 99.6% recall, and 99.7% precision, the entire HBbDNPF model—which incorporates cloud masking, spectral band normalisation, NDVI/NDWI indexes, PCA-based dimensionality reduction, and HBO—achieves the greatest metrics. Eliminating specific steps results in appreciable drops in accuracy. For instance, deleting cloud masking lowers accuracy to 96.1%, while deleting PCA lowers accuracy to 94.9% and increases memory use from 2.5 GB to 3.1 GB because the input features are more dimensional. The significance of their impact on improving vegetation signal and reducing sensor bias is demonstrated by the decrease in accuracy ($\approx$95.1–95.6%) resulting from the absence of spectral band normalisation or NDVI/NDWI indexes. 95.2% accuracy is obtained by removing HBO while maintaining all feature-engineering procedures, demonstrating the usefulness of HBO in maximising model parameters. With an accuracy of 91.5%, the baseline DNN, with no feature engineering or HBO, performs the poorest, suggesting that the synergy between feature engineering stages and HBO drives the model's higher performance. Furthermore,

training time and memory consumption measurements demonstrate that feature engineering, especially PCA, improves accuracy while reducing computational costs and increasing pipeline efficiency.

Table 12. Ablation study of HBO

Model Variant / Setting	Cloud Masking	Spectral Band Normalisation	NDVI/NDWI Indices	PCA Dimensionality Reduction	Accuracy % (Mean ± SD)	Recall % (Mean ± SD)	Precision % (Mean ± SD)	F1-Score % (Mean ± SD)	Training Time (s)	Memory Usage (GB)
HBbDNPF	✓	✓	✓	✓	99.9 ± 0.3	99.6 ± 0.4	99.7 ± 0.3	99.65 ± 0.3	180	2.5
No Cloud Masking (Other Steps + HBO)	✗	✓	✓	✓	96.1 ± 0.4	96.0 ± 0.5	96.1 ± 0.4	96.05 ± 0.4	175	2.6
No Spectral Band Normalisation (Other Steps + HBO)	✓	✗	✓	✓	95.6 ± 0.4	95.4 ± 0.5	95.5 ± 0.4	95.45 ± 0.4	173	2.6
No NDVI/NDWI Indices (Other Steps + HBO)	✓	✓	✗	✓	95.1 ± 0.5	94.8 ± 0.5	95.0 ± 0.5	94.9 ± 0.5	170	2.6
No PCA Dimensionality Reduction (Other Steps + HBO)	✓	✓	✓	✗	94.9 ± 0.5	94.6 ± 0.5	94.8 ± 0.5	94.7 ± 0.5	200	3.1
No HBO (All Feature-Engineering Steps Only)	✓	✓	✓	✓	95.2 ± 0.4	95.0 ± 0.5	95.3 ± 0.4	95.1 ± 0.4	130	2.1
Baseline DNN (No HBO, No Feature-Engineering)	✗	✗	✗	✗	91.5 ± 0.6	91.2 ± 0.5	91.3 ± 0.6	91.25 ± 0.6	110	2.0

5.4.3. Ethical implications Although the HBbDNPF architecture exhibits excellent computational efficiency and prediction accuracy, several practical and ethical issues arise with its use. Concerns about data privacy may arise from a moral perspective when UAV spectral data is collected over private farms, particularly for smallholder farmers who may not want to share information about their crop health or productivity. To preserve farmer privacy, it is essential to guarantee informed permission, safe data storage, and anonymisation of farm-specific data. The cost of UAV hardware and sensors, which may be too expensive for small or resource-constrained farms, as well as the technical expertise required to fly drones, preprocess spectral data, and interpret model outputs, are practical obstacles to implementation. Weather variations, flight restrictions, and maintenance needs are additional

difficulties that may impact data quality and model dependability. Future research could investigate low-cost options, such as incorporating satellite imagery, Internet of Things soil and climate sensors, or community-shared UAV services, to mitigate these obstacles. Additionally, user-friendly interfaces and automated pipelines could be developed to make the technology available to a broader range of farmers.

Real-world pilot study

Pilot studies with farmers in the real world are crucial to verifying the HBbDNPF framework's usability and practical impact. This research would use the HBbDNPF model to estimate yield, deploy UAVs to gather spectral data over real fields, and provide farmers with actionable insights almost instantly. Diverse farm sizes, crop varieties, and geographical areas should be included in pilot programs to evaluate the system's performance under various operational and environmental conditions. Prediction accuracy in operational contexts, farmer-friendly model output interpretation, promptness of recommendations, and perceived value in decision-making are essential evaluation indicators. The user interface, training materials, and data collection procedures can all be improved based on input from these pilot projects. Iterative cooperation with farmers would also aid in identifying real-world issues, such as scheduling UAV flights, local laws, and integrating the system with existing farm management techniques. This would ensure that the system is not only technically accurate but also practical and adaptable in real-world agricultural settings.

6. Conclusion

This study introduces the Honey Badger-based Deep Neural Predictive Framework (HBbDNPF), which utilises features derived from UAV spectral data to predict agricultural yields. Before preprocessing to eliminate noise and guarantee high-quality input, the workflow started with gathering and training on the UAV dataset. In the feature analysis stage, pertinent features were retrieved and applied to predict crop yield. A variety of crop kinds, including wheat, maise, mustard, rapeseed, barley, onion, bajra, and jowar, were classified by the model. According to performance evaluation, HBbDNPF significantly outperforms traditional approaches, achieving 99.99% accuracy, 99.97% recall rate, and 99.95% precision. With an MAE of 0.15 and RMSE of 0.17, error measures were also significantly decreased, demonstrating the accuracy and dependability of the framework.

The suggested approach maintains computing efficiency while providing extremely accurate and consistent crop yield estimates by combining temporal UAV spectral data, Honey Badger optimisation, and robust feature selection. These outcomes highlight the model's potential for real-world uses in resource efficiency and precision agriculture.

6.1. Limitation

Although encouraging, the study had a few drawbacks. The model may not accurately reflect the variability found in actual agricultural contexts because it was tested using a particular UAV spectral dataset. As a result, until the excellent performance is confirmed on more varied and openly accessible datasets, it should be regarded with caution. Furthermore, the framework may not be as applicable in environments with variable sensor quality or environmental limitations due to its dependence on high-quality UAV data and well-preprocessed features. To further enhance predictive robustness, future studies should focus on verifying the framework across diverse datasets, exploring various remote sensing data sources, and refining the HBA-DNN integration. By taking these actions, the actual potential of the HBA-DNN synergy in realistic agricultural yield forecasting will be verified.

REFERENCES

1. Z. Chen, Y. Xu, J. Ge & G. Chen, *Exploring the value of Dioscorea melanophyma: an orphan crop from China*, Ind. Crop. Prod, Vol. 223, pp. 120136, 2025.
2. V.R.R. Kolipaka, A. Namburu, *An automatic crop yield prediction framework designed with two-stage classifiers: a meta-heuristic approach*, Multimed Tools Appl, Vol. 83, pp. 28969–28992, 2024.
3. K. Venkatesh, K.J. Naik, *An ensemble transfer learning for nutrient deficiency identification and yield-loss prediction in crop*, Multimed Tools Appl, 2024.

4. E. Vidya Madhuri, J.S. Rupali, S.P. Sharan, N. Sai Pooja, G.S. Sujatha, D.P. Singh & R. Prabha, *Transforming pest management with artificial intelligence technologies: The future of crop protection*, Journal J. Crop Health, Vol. 77, No. 2, pp. 48, 2024.
5. C.B. Adams, C. Neely & R. Graebner, *Yield variation, plasticity, adaptation, and performance ranking of winter wheat varieties across the environmental gradient of the US Pacific Northwest*, Crop Sci, Vol. 65, No. 1, pp. e70018, 2025.
6. M.H.M. Saad, N.M. Hamdan, M.R. Sarker, *State of the art of urban smart vertical farming automation system: advanced topologies, issues and recommendations*, Electron, Vol. 10, No. 12, pp. 1422, 2024.
7. M. Javaid, A. Haleem, I.H. Khan, R. Suman, *Understanding the potential applications of Artificial Intelligence in Agriculture Sector*, Adv Agrochem, Vol. 2, No. 1, pp. 15-30, 2023.
8. N. Biswakarma, R.R. Zhiipao, N.C. Gulleibi, K. Baishya, N. Talukdar, B. Makdoh & V.K. Mishra, *Integrated crop management practices for rice: impact on crop growth, yield, nutrient acquisition, water productivity, and farm profitability*, Paddy Water Environ, pp. 1-15, 2025.
9. H.A.A. Gaznayee, S.H. Zaki, A.M.F. Al-Quraishi, *Integrating remote sensing techniques and meteorological data to assess the ideal irrigation system performance scenarios for improving crop productivity*, Water, Vol. 15, No. 8, pp. 1605, 2023.
10. N. Bali, A. Singla, *Emerging trends in machine learning to predict crop yield and study its influential factors: A survey*, Arch Comput Methods Eng, Vol. 29, No. 1, pp. 95-112, 2022.
11. N. Delavarpour, C. Koparan, J. Nowatzki, S. Bajwa, X. Sun, *A technical study on UAV characteristics for precision agriculture applications and associated practical challenges*, Remote Sens, Vol. 13, No. 6, pp. 1204, 2021.
12. A. Nabavi-Pelesaraei, S. Rafiee, F. Hosseini-Fashami, K.W. Chau, *Artificial neural networks and adaptive neuro-fuzzy inference system in energy modeling of agricultural products*, In Predictive modelling for energy management and power systems engineering, pp 299-334, 2021.
13. M. Qiao, X. He, X. Cheng, P. Li, K. Zheng, M. Xu & Y. Chen, *Spatial-temporal cross-view contrast for self-supervised crop yield prediction*, Expert Syst. Appl, pp. 128036, 2021.
14. S. Ahmad, *Information and communication technologies in sustainable crop protection: advancing towards sustainable agriculture*, Proc. Indian Natl. Sci. Acad, pp. 1-11, 2025.
15. B. Bali, Z.N. Ngida, I. Habila & I. Goni, *Artificial Intelligence Applied in Optimization of Crop Yield for Ensuring Food Security in Nigeria: A Systematic Analysis*, SNCS, Vol. 6, No. 5, pp. 483, 2025.
16. U. Nirosha & G. Vennila, *Enhancing crop yield prediction for agriculture productivity using federated learning integrating with graph and recurrent neural networks model*, Expert Syst. Appl, pp. 128312, 2025.
17. P. Muruganantham, S. Wibowo, S. Grandhi, N.H. Samrat, N. Islam, *A systematic literature review on crop yield prediction with deep learning and remote sensing*, Remote Sens, Vol. 14, No. 9, pp. 1990, 2022.
18. N.N. Purohit, R.K. Ghosh, A.J. Price & A. Maity, *Potential ecological implications of extensive cereal rye cover cropping in the United States*, Crop Sci, Vol. 65, No. 3, pp. e70056, 2025.
19. M. Qiao, X. He, X. Cheng, P. Li, H. Luo, L. Zhang, Z. Tian, *Crop yield prediction from multispectral, multi-temporal remotely sensed imagery using recurrent 3D convolutional neural networks*, Int J Appl Earth Obs Geoinf, Vol. 102, pp. 102436, 2021.
20. R. Bhardwaj, A. Yadav, A. Sahoo, P. Kumari, L.A. Singh, P. Swapnil & S. Kumar, *Microalgal-based sustainable bio-fungicides: a promising solution to enhance crop yield*, Discov. Sustain, Vol. 6, No. 1, pp. 39, 2025.
21. P. Abbaszadeh, K. Gavahi, A. Alipour, P. Deb, H. Moradkhani, *Bayesian multi-modeling of deep neural nets for probabilistic crop yield prediction*, Agr Forest Meteorol, Vol. 314, pp. 108773, 2022.
22. M. Yli-Heikkilä, S. Wittke, M. Luotamo, E. Puttonen, M. Sulkava, P. Pellikka, A. Klami, *Scalable crop yield prediction with Sentinel-2 time series and temporal convolutional network*, Remote Sens, Vol. 14, No. 17, pp. 4193, 2022.
23. M. Kuradusenge, E. Hitimana, D. Hanyurwimfura, P. Rukundo, K. Mtonga, A. Mukasine, A. Uwamahoro, *Crop yield prediction using machine learning models: Case of Irish potato and maise*, Agricu, Vol. 13, No. 1, pp. 225, 2023.
24. G. Shuai, B. Basso, *Subfield maize yield prediction improves when in-season crop water deficit is included in remote sensing imagery-based models*, Remote Sens Environ, Vol. 272, pp. 112938, 2022.
25. J. Wang, H. Si, Z. Gao, L. Shi, *Winter wheat yield prediction using an LSTM model from MODIS LAI products*, Agric, Vol. 12, No. 10, pp. 1707, 2022.
26. A. Gafurov, S. Mukharamova, A. Saveliev, O. Yermolaev, *Advancing Agricultural Crop Recognition: The Application of LSTM Networks and Spatial Generalization in Satellite Data Analysis*, Agric, Vol. 13, No. 9, pp. 1672, 2023.
27. U. Bhimavarapu, G. Battineni, N. Chintalapudi, *Improved optimisation algorithm in LSTM to predict crop yield*, Computers, Vol. 12, No. 1, pp. 10, 2023.
28. D. Elavarasan, P.M. Durai Raj Vincent, *Fuzzy deep learning-based crop yield prediction model for sustainable agronomical frameworks*, Neural Comput Appl, Vol. 33, No. 20, pp. 13205-13224, 2021.
29. A. Rajagopal, S. Jha, M. Khari, S. Ahmad, B. Alouffi, A. Alharbi, *A novel approach in prediction of crop production using recurrent cuckoo search optimisation neural networks*, Appl Sci, Vol. 11, No. 21, pp. 9816, 2021.
30. X. Jin, Y. Sun, J. Che, M. Bagavathiannan, J. Yu, Y. Chen, *A novel deep learning-based method for detection of weeds in vegetables*, Pest Manag Sci, Vol. 78, No. 5, pp. 1861-1869, 2022.
31. A. Tripathi, R.K. Tiwari, S.P. Tiwari, *A deep learning multi-layer perceptron and remote sensing approach for soil health based crop yield estimation*, Int J Appl Earth Obs Geoinf, Vol. 113, pp. 102959, 2022.
32. L. Jovanovic, M. Zivkovic, N. Bacanin, M. Dobrojevic, V. Simic, K.K. Sadasivuni, E.B. Tirkolaee, *Evaluating the performance of metaheuristic-tuned weight agnostic neural networks for crop yield prediction*, EURAL COMPUT APPL, Vol. 10, pp. 1-30, 2023.
33. C. Kumar, P. Mubvumba, Y. Huang, J. Dhillon, K. Reddy, *Multistage corn yield prediction using high-resolution UAV multispectral data and machine learning models*, Agronomy, Vol. 13, No. 5, pp. 1277, 2023.
34. S. Fei, M.A. Hassan, Y. Xiao, X. Su, Z. Chen, Q. Cheng, F. Duan, R. Chen, Y. Ma, *UAV-based multi-sensor data fusion and machine learning algorithm for yield prediction in wheat*, Precis. Agric, Vol. 24, No. 1, pp. 187-212, 2023.
35. J. Skobalski, V. Sagan, H. Alifu, O. Al Akkad, F.A. Lopes, F. Grignola, *Bridging the gap between crop breeding and GeoAI: Soybean yield prediction from multispectral UAV images with transfer learning*, ISPRS J. Photogramm. Remote Sens, Vol. 210, pp. 260-81, 2024.